HHS Public Access

Author manuscript

Food Chem Toxicol. Author manuscript; available in PMC 2017 December 01.

Published in final edited form as:

Food Chem Toxicol. 2016 December ; 98(Pt B): 107–118. doi:10.1016/j.fct.2016.10.021.

Differential Susceptibility to Acetaminophen-Induced Liver Injury in Sub-Strains of C57BL/6 Mice: 6N versus 6J

Luqi Duan[a], **John S. Davis**[b,1], **Benjamin L. Woolbright**[a], **Kuo Du**[a], **Mala Chakraborty**[b,2], **James Weemhoff**[a], **Hartmut Jaeschke**[a,*], and **Mohammed Bourdi**[b,3]

[a]Department of Pharmacology, Toxicology & Therapeutics; Kansas City, KS, 66160

[b]Molecular and Cellular Toxicology Section, Laboratory of Molecular Immunology, National Heart, Lung and Blood Institute, National Institutes of Health, Bethesda, MD, 20850.

Abstract

Mouse models of acetaminophen (APAP) hepatotoxicity are considered relevant for the human pathophysiology. The C57BL/6 strain is most popular because it is the background strain of gene knock-out mice. However, conflicting results in the literature may have been caused by sub-strain mismatches, e.g. C57BL/6J and C57BL/6N. This study was initiated to determine the mechanism behind the sub-strain susceptibility to APAP toxicity. C57BL/6N and C57BL/6J mice were dosed with 200 mg/kg APAP and sacrificed at different time points. C57BL/6N mice developed significantly more liver injury as measured by plasma ALT activities and histology. Although there was no difference in glutathione depletion or cytochrome P450 activity between groups, C57BL/6N had a higher glutathione disulfide-to-glutathione ratio and more APAP protein adducts. C57BL/6N showed more mitochondrial translocation of phospho-JNK and BAX, and more release of mitochondrial intermembrane proteins (apoptosis-inducing factor (AIF), second mitochondria-derived activator of caspases (SMAC), which caused more DNA fragmentation. The increased mitochondrial dysfunction was confirmed *in vitro* as C57BL/6N hepatocytes had a more precipitous drop in JC-1 fluorescence after APAP exposure. Conclusion: C57BL/6N mice are more susceptible to APAP-induced hepatotoxicity, likely due to increased formation of APAP-protein adducts and a subsequent enhancement of mitochondrial dysfunction associated with aggravated nuclear DNA fragmentation.

[*]**Correspondence:** Hartmut Jaeschke, PhD, Department of Pharmacology, Toxicology & Therapeutics, University of Kansas Medical Center, 3901 Rainbow Blvd, MS 1018, Kansas City, KS, 66160 USA, Phone: +1 913 588 7969 Fax: +1 913 588 7501, hjaeschke@kumc.edu.

lduan@kumc.edu; John.Davis@nih.gov; bwoolbright@kmc.edu; kdu@kumc.edu; mala.cahkraborty@nih.gov; jweemhoff@kumc.edu; mohammed.bourdi@nih.gov

[1]Experimental Transplantation and Immunology Branch, National Cancer Institute, National Institutes of Health, Bethesda, MD

[2]Hematology Branch, National Heart Lung and Blood Institute, National Institutes of Health, Bethesda, MD

[3]Division of Pre-Clinical Innovation, National Center for Advancing Translational Sciences, National Institutes of Health, Bethesda, MD

Conflict of Interest

The authors report no conflict of interest.

Keywords

acetaminophen hepatotoxicity; C57BL/6 sub-strains; mitochondrial dysfunction; protein adducts; DNA fragmentation

1. INTRODUCTION

Acetaminophen (APAP)-induced liver injury remains a leading cause of drug-induced hepatotoxicity in western societies (Lee, 2013). During an acute overdose, a small portion of APAP is rapidly converted to the reactive metabolite *N*-acetyl-p-benzoquinone imine (NAPQI) by cytochrome P450 enzymes, such as CYP2E1 (Nelson, 1990; Bessems and Vermeulen, 2001). Although NAPQI can be detoxified by glutathione (GSH), it also forms protein adducts (Cohen et al., 1997). Adducts of mitochondrial proteins are thought to cause the initial oxidant stress in the mitochondria that leads to activation of redox-sensitive MAP kinases and ultimately to phosphorylation of c-jun-N-terminal kinase (JNK) (Han et al., 2013; Jaeschke et al., 2012; McGill and Jaeschke 2013). This oxidative stress is amplified by translocation of phospho-JNK to the mitochondria (Hanawa et al., 2008; Saito et al., 2010). The mitochondrial oxidant stress and peroxynitrite formation (Cover et al., 2005) are mainly responsible for the opening of the mitochondrial permeability transition (MPT) pore and collapse of the membrane potential (Kon et al., 2004). A consequence of the MPT is mitochondrial swelling and rupture of the outer membrane, which causes the release of intermembrane membrane proteins, such as apoptosis-inducing factor (AIF), endonuclease G, and the second mitochondria-derived activator of caspases (SMAC), into the cytoplasm of the cell (Jaeschke et al., 2012). AIF and endonuclease G can then translocate to the nucleus where they cause extensive DNA fragmentation (Bajt et al., 2006). Both mitochondrial dysfunction and nuclear DNA damage are the cause of extensive necrotic cell death after APAP overdose (Gujral et al., 2002). Cell necrosis then results in the release of many cellular constituents including mitochondrial and nuclear DNA, mitochondrial enzymes, high mobility group box 1 (HMGB1) protein, cytokeratin-18, miRNA-122, and many more (Antoine et al., 2012, 2013; Beger et al., 2015; McGill et al., 2012, 2014; McGill and Jaeschke, 2014).

Progress in the understanding of APAP hepatotoxicity mechanisms is facilitated by the widespread use of genetic mouse models such as gene knockout mice as an experimental tool. These knockout animals are typically generated on, or are later backcrossed to, popular mouse background strains such as the C57BL/6 mouse, a strain readily available from various commercial sources. However, subtle genetic differences have developed in sub-strains of C57BL/6 mice from different sources that can have a substantial impact on experiments (Simon et al., 2013). In fact, there was a controversy regarding the role of JNK2 in APAP hepatotoxicity with groups reporting that JNK2-deficient mice were protected (Gunawan et al., 2006), not affected (Henderson et al., 2007; Saito et al., 2010), or even showed aggravation of APAP-induced liver injury (Bourdi et al., 2008). A follow-up study demonstrated that the main reason for the controversial results may have been the use of wild type animals from different C57BL/6 sub-strains (Bourdi et al., 2011). These findings raised the concern that some problems with reproducibility of research results today could

come from the unrecognized mismatch of wild type and gene knock-out animals from different background sub-strains. Since C57BL/6N mice are considerably more susceptible to APAP overdose than C57BL/6J mice (Bourdi et al., 2011), the objective of this investigation was to assess whether this enhanced susceptibility was caused by different injury mechanisms in these sub-strains. However, this objective of understanding the mechanism of APAP-induced cell death in various C57BL/6 sub-strains should not be confused with the variable toxicity of APAP in different mouse strains, which is a well-known phenomenon (Harrill et al., 2009a,b).

2. MATERIALS AND METHODS

2.1 Animal Protocols

Male C57BL/6J mice (Stock # 000664; Jackson Laboratories, Bar Harbor, Maine, USA) and male C57BL/6NCr mice (Strain Code: 556; Charles River, NCI Research Models and Services, Frederick, Maryland, USA) were purchased from the respective vendor at 8-10 weeks of age and acclimated in our facility for at least 5 days. Experimental protocols were approved by the local Institutional Animal Care and Use Committee before the onset of experimentation. All animals were fasted overnight and then treated with 200 mg/kg APAP diluted in warm saline via an i.p. injection. This dose was based on our preliminary data that indicated the 300mg/kg dose caused substantial mortality in the C57BL/6N sub-strain, which prevented robust comparison between the sub-strains (data not shown). At the indicated time points, groups of mice were sacrificed via cervical dislocation and exsanguination via the hepatic vena cava. Heparinized blood was collected and centrifuged at 14,000 $\times g$ for 3 minutes to collect plasma. Liver was resected and snap frozen in liquid nitrogen or stored in 4% paraformaldehyde for 24 hours for histology.

2.2 Biochemical Measurements

Plasma alanine aminotransferase (ALT) activities were measured via the Point Scientific ALT test (Point Scientific Inc., Canton, MI) per the manufacturer's instruction. Total glutathione or glutathione disulfide (GSSG) were measured with a modified Tietze assay as previously described (Jaeschke and Mitchell, 1990). Cytochrome P450 activity was measured using 7-ethoxy-4-trifluoromethylcoumarin (7-EFC) as described previously (Ramachandran et al., 2011). In brief, liver homogenates were incubated with 50 μM 7-EFC and 1 mM NADPH, in 0.1 M PBS (pH 7.4) and DMSO-inhibitable 7-EFC fluorescence was measured. This substrate detects mainly CYP2E1 and CYP1A2 activities (Buters et al., 1993), which are the main cytochrome P450 enzymes responsible for the metabolic activation of APAP (Zaher et al., 1998).

2.3 Histology and Immunohistochemistry

Tissue was fixed and embedded in paraffin. Hematoxylin and eosin (H&E) staining was performed for evaluation of the area of necrosis as described (Gujral et al., 2002). TUNEL staining was performed for evaluation of nuclear DNA damage per the manufacturer's instructions (Roche Diagnostics, Basel, Switzerland).

2.4 Western Blotting

Snap frozen tissue was homogenized in a CHAPs containing protein buffer and total protein was measured using the BCA assay (Pierce Scientific, Waltham, MA). Gel electrophoresis was carried out on protein lysates from individual samples, which were then transferred to a nitrocellulose blot. Densitometry was performed to quantitatively assess differences using Image J software. In brief, densitometry was performed serially on blots and normalized to either the non-phosphorylated form (JNK) or the loading control, either porin or beta-actin. Antibodies to total JNK (catalogue #9252), phospho-JNK (# 9251), β-actin (#4970), BAX (#27742), MLK-3 (#2817) and AIF (#5318) were purchased from Cell Signaling Technologies (Danvers, MA). Sab and ASK-1 were obtained from Santa Cruz (sc-10167 and sc-7931) and SOD2 was acquired from Millipore (06-984). The antibodies against thioredoxin 2 (ab16836), Cyp2E1 (ab28146) and porin (#14734) were purchased from Abcam (Cambridge, UK). SMAC (# 612245) was acquired from BD Biosciences (San Diego, CA).

2.5 Acetaminophen Protein Adduct Measurements

APAP protein adducts were measured as described (Ni et al., 2012b). Briefly, low molecular weight compounds were removed from the liver homogenate via Bio-spin 6 columns (Bio-Rad, Hercules, CA) and subsequently the protein fraction was digested with proteases to liberate APAP-CYS conjugates. The conjugates were measured using high performance liquid chromatography with electrochemical detection (HPLC-ED) as described (Muldrew et al., 2002).

2.6 Statistics

Data are expressed as means ± SE. Comparison between two groups were performed with Student's *t*-test. Comparisons between multiple groups were performed using one-way ANOVA followed by Student-Neuman-Keuls post hoc test for multiple groups. $p<0.05$ was considered significant.

3. RESULTS

3.1 C57BL/6N mice are more sensitive to APAP-induced liver injury than C57BL/6J mice

Data from our previous studies indicated that sub-strains of C57BL/6 mice might have differential susceptibility to APAP overdose (Bourdi et al., 2011). To confirm this, C57BL/6N or C57BL/6J mice were fasted, treated with 200 mg/kg APAP, and sacrificed over a series of time points. C57BL/6N mice were significantly more susceptible to APAP hepatotoxicity as evidenced by increased plasma ALT values at both 2 h and 8 h after APAP overdose (Figure 1A). These data were confirmed by both H&E and TUNEL staining (Figure 1B,C). The histology indicated that C57BL/6N mice had extensive centrilobular hepatocellular necrosis at 8 h after APAP overdose, whereas only limited cell death was present in the C57BL/6J mice. TUNEL staining confirmed these findings. DNA fragmentation in the centrilobular area was substantially more extensive in C57BL/6N compared to C57BL/6J mice (Figure 1C).

3.2 APAP metabolism is similar in C57BL/6N and C57BL/6J mice

To determine if the increased susceptibility to APAP overdose was due to differences in metabolism between the sub-strains, hepatic GSH depletion and recovery was compared in C57BL/6J versus C57BL/6N mice after APAP administration. Both depletion of GSH and its regeneration were similar between sub-strains (Figure 2A). In contrast, C57BL/6N mice had significantly higher levels of glutathione disulfide (GSSG) 8 h after APAP overdose (Figure 2B), and a higher GSSG-to- GSH ratio at the same time point (Figure 2C), indicative of increased oxidative stress in the C57BL/6N mouse. To confirm these data, protein-derived APAP-CYS adducts were measured at 30 min, 2 h and 8 h after APAP administration. C57BL/6N mice accumulated more APAP-CYS adducts in the total liver homogenate 2h and 8 h after APAP administration (Figure 3A). There was also an increase in mitochondrial adducts at 2 h (Figure 3B), which is the peak of adduct formation (McGill et al., 2013). This was in spite of the fact that P450 enzyme activities were similar between the sub-strains of mice (Figure 3C). To ascertain if some of these differences might be due to differential expression of proteins involved in metabolism or antioxidant response, we also assessed baseline expression of CYP2E1, superoxide dismutase 2 (SOD2) and thioredoxin 2 (Trx2); however, no difference was observed in the expression of these proteins when control mice of each sub-strain were compared (Supplemental Figure 1). Despite the relatively similar GSH depletion and recovery profiles, the increased APAP-CYS adduct formation in the C57BL/6N sub-strain indicates a reduced rate of detoxification of APAP in C57BL/6N mice. This may be a cause of the increased oxidative stress and exacerbated injury in this sub-strain.

3.3 Enhanced mitochondrial JNK translocation in C57BL/6N mice

JNK is an established intracellular mediator of APAP-induced liver injury in both mice (Gunawan et al., 2006; Hanawa et al., 2008; Saito et al., 2010) and in humans (Xie et al., 2014). Given the importance of mitochondrial JNK translocation to APAP toxicity, JNK activation (phosphorylation) and mitochondrial translocation was measured in C57BL/6N and C57BL/6J mice after an APAP overdose. Interestingly, there was increased phospho-JNK translocation in C57BL/6N 2 h after APAP overdose as compared to C57BL/6J mice (Figure 4A, C), when compared to the mitochondrial reference protein porin; however, there was also increased total JNK in the mitochondria of C57BL/6N mice (Figure 4A,C). Furthermore, there was an increase in cytoplasmic phospho-JNK expression and increased activation in C57BL/6N as compared to C57BL/6J mice (Figure 4B,D). To confirm the increase in JNK pathway involvement, we also measured protein expression of JNK pathway members mixed lineage kinase-3 (MLK3) (Sharma et al., 2012), apoptosis signal regulating kinase 1 (ASK1) (Xie et al., 2015b), and SH3BP5 binding protein (Sab) (Win et al., 2011). While there was no expression in upstream JNK activators ASK-1 or MLK-3, there was increased Sab expression at 2h in C57BL/6N mice consistent with increased mitochondrial JNK translocation (Supplemental Figure 2). These data indicate that C57BL/6N mice have increased JNK activation in the cytosol after APAP overdose resulting in increased mitochondrial translocation, which may contribute to the higher injury observed in the C57BL/6N mice.

3.4 Enhanced mitochondrial BAX translocation and release of both AIF and SMAC in C57BL/6N mice

As it was previously noted there was increased DNA damage in the C57BL/6N mice (Figure 1C) as well as enhanced mitochondrial JNK translocation (Figure 4A,C), we measured translocation and release of a number of potential mitochondrial mediators. Upon APAP exposure, the Bcl-family member BAX translocates to the mitochondria and enhances the permeability of the outer mitochondrial membrane through formation of pores and causes release of intermembrane proteins (Bajt et al., 2008). While cytoplasmic BAX levels were similar between groups (Figure 5A), increased BAX translocation to the mitochondria was observed in C57BL/6N mice at both 2 h and 8 h after APAP overdose as compared to the C57BL/6J sub-strain (Figure 5B), despite similar control levels. To observe potential downstream mediators of the enhanced BAX translocation, release of AIF from the mitochondria into the cytosol was measured in both strains of mice. C57BL/6N mice had significantly increased AIF release into the cytosol as compared to C57BL/6J mice at both 2 h and 8 h after APAP overdose (Figure 6A); again, baseline levels of AIF were similar in both sub-strains. Interestingly, AIF protein expression was induced in C57BL/6N mice as indicated by significantly higher mitochondrial levels of AIF after APAP treatment (Figure 6B). Release of AIF and other proteins such as endonuclease G from the mitochondria to the cytoplasm and subsequent translocation to the nucleus is responsible for DNA fragmentation as indicated by the TUNEL assay (Bajt et al., 2006, 2011). Thus, the enhanced DNA damage in C57BL/6N mice is likely caused at least in part by the increased mitochondrial BAX translocation and the subsequent higher release of intermembrane proteins, e.g. AIF, some of which can translocate to the nucleus and promote DNA fragmentation. In order to confirm the higher outer membrane permeability increase in C57BL/6N mice, the release of another mitochondrial intermembrane protein, SMAC, was investigated both in the mitochondria and the cytosol. C57BL/6N had increased levels of cytosolic SMAC both 2 h and 8 h after APAP-induced liver injury as compared to C57BL/6J mice (Figure 7A) although mitochondrial levels were similar both before and after APAP treatment (Figure 7B). These data confirm the increased outer membrane permeability in C57BL/6N mice after APAP overdose. Of note, cytosolic SMAC levels were significantly higher in untreated C57BL/6N mice (Figure 8A,C). However, no differences were found between C57BL/6N and C57BL/6J mice with regard to baseline cytosolic AIF or BAX levels (Figure 8A,B,D).

3.5 Primary hepatocytes from C57BL/6N mice develop mitochondrial dysfunction faster than cells from C57BL/6J mice

To confirm the enhanced mitochondrial instability, we isolated primary hepatocytes from mice and exposed them to a cytotoxic concentration of APAP. Hepatocytes of C57BL/6N mice had a much sharper decrease in JC-1 fluorescence when exposed to 5 mM APAP for 3 h (Figure 9A) indicating enhanced susceptibility to APAP-mediated mitochondrial dysfunction. At a later time point when substantial LDH release had occurred (9 h), there was little difference in the loss of the mitochondrial membrane potential or the degree of cellular LDH release between hepatocytes of C57BL/6N and C57BL/6J mice (Figure 9A,B). This suggests that with this concentration of APAP, mitochondrial dysfunction is mainly accelerated in hepatocytes of C57BL/6N mice, but not fundamentally different compared to hepatocytes of C57BL/6J mice. As such, sufficient mitochondrial dysfunction is present *in*

vitro to induce cell death for both sub-strains despite the more rapid acceleration in C57BL/6N mice.

4. DISCUSSION

The objective of this investigation was to better understand sub-strain differences in the susceptibility to APAP overdose between C57BL/6N and C57BL/6J mice. Our study confirmed that C57BL/6N mice had more severe liver injury in response to a toxic dose of APAP (Bourdi et al., 2011). It is important to point out that we used the C57BL/6NCr strain from Charles River whereas in our previous study we used C57BL/6NJ from Jackson Laboratories (Bourdi et al., 2011). Despite the different vendors, C57BL/6N mice from both sources proved to be more susceptible compared to the C57BL/ 6J sub-strain. Recognizing the sub-strain of knockout mice and comparing them to the proper wild type mice is critical for the correct interpretation of experimental data (Fontaine and Davis, 2016). As shown by investigations into the role of JNK2 in APAP toxicity, sub-strain mismatch can lead to contradicting and irreproducible results (Bourdi et al., 2008, 2011; Gunawan et al., 2006; Henderson et al., 2007; Saito et al., 2010). This difference in hepatotoxicity does not only apply to APAP overdose but also to a mechanistically different model of T-cell-dependent liver injury after concanavalin A treatment (Bourdi et al., 2011). Importantly, the concanavalin A model uses fed mice, suggesting that the nutritional status does not affect the different susceptibility of the two sub-strains to the liver toxins.

4.1 Differential response of C57BL/6 sub-strains to APAP overdose

Over the last several decades, a number of critical events in the mechanism of APAP-induced cell death have been established (Jaeschke et al., 2012; McGill and Jaeschke, 2013). After an overdose of APAP, excessive formation of the reactive metabolite NAPQI leads to hepatic GSH depletion and protein adduct formation (Jollow et al., 1973; Mitchell et al., 1973a,b; Dahlin 1984). Mitochondrial protein adduct formation (Tirmenstein and Nelson, 1989; Xie et al., 2015a), JNK activation (Hanawa et al., 2008; Hu et al., 2016) and eventually MPT (Kon et al., 2004) are key events of the observed toxicity. In addition, early BAX translocation to mitochondria results in outer membrane permeabilization (Bajt et al., 2008), or later MPT-induced matrix swelling and rupture of the outer membrane. This leads to the release of the intermembrane proteins AIF and endonuclease G into the cytosol and translocation of these proteins to the nucleus, where they contribute to nuclear DNA fragmentation (Cover et al., 2005), which is a hallmark of APAP-induced cell death (Ray et al., 1990). Mitochondrial oxidant stress and peroxynitrite formation are central to mitochondrial dysfunction and toxicity (Jaeschke, 1990; Cover et al., 2005). Using a moderate overdose of 200 mg/kg, which is tolerated by both sub-strains of mice without mortality, allows for direct comparison of the mechanism over time. Our data indicate that the mechanism of toxicity involves all the described events in both sub-strains. However, C57BL/6N mice consistently showed more severe mitochondrial dysfunction. In fact, all parameters indicating mitochondrial dysfunction (JNK, P-JNK, GSSG, BAX, Sab) and downstream events like mitochondrial AIF and SMAC release and DNA fragmentation were consistently more elevated in C57BL/6N compared to C57BL/6J mice. This more severe mitochondrial dysfunction in C57BL/6N mice correlated with the more severe cell injury in

these mice. However, the observation that all parameters of mitochondrial dysfunction were enhanced in both sub-strains and the difference between C57BL/6N and C57BL/6J mice was mainly quantitative suggests that the overall mechanism of APAP toxicity is the same and that the reason for the difference is upstream of mitochondria.

4.2 Protein adduct formation and mitochondrial instability during APAP hepatotoxicity

During an acute overdose, APAP is rapidly metabolized by cytochrome P450 enzymes into the reactive metabolite NAPQI (Dahlin et al., 1984), which quickly adducts nearby proteins and leads to considerable oxidative stress (reviewed in Jaeschke et al., 2012). Glutathione depletion typically functions as a standard marker of APAP metabolism, as NAPQI rapidly binds glutathione and the APAP-GSH conjugate is then excreted (Rosen et al., 1984). Of note, we found neither a difference (between the two sub-strains) in the time course of glutathione depletion and recovery, nor any difference in P450 activity (mainly Cyp2E1 and Cyp1A2), but substantial differences in APAP-CYS adduct levels both in the total homogenate, as well as in the mitochondrial fraction were observed. APAP-CYS adduct are the most direct biomarkers of differences in the metabolic activation of APAP. APAP-protein adducts, especially in mitochondria, are widely thought to be the initiating event for mitochondrial oxidant stress and dysfunction that is responsible for eventual cell death (Jaeschke et al., 2012). Thus, the higher degree of APAP-protein adduct formation in C57BL/6N mice may explain the higher susceptibility to APAP overdose of this sub-strain.

Another difference between C57BL/6J and C57BL/6N mice, although beyond the scope of the present paper, could be a difference in autophagy. Both damaged mitochondria (Ni et al., 2012a) and protein adducts (Ni et al., 2016) were shown to be removed by autophagy, an adaptive mechanism that protects against APAP hepatotoxicity. The consistently lower adducts in C57BL/6J mice could be caused by the reduced formation of adducts compared to C57BL/6N mice or could be the result of higher autophagic clearance. The latter explanation would be consistent with the fact that no significant difference in drug metabolizing enzyme activity was found. More experiments need to be done to investigate this mechanism in more detail.

Consistent with the findings of increased mitochondrial dysfunction *in vivo*, cells isolated from C57BL/6N mice also showed a more rapid loss of the mitochondrial membrane potential *in vitro* in response to APAP exposure for 3 h. However, at the later time point (9 h) when cell death occurred, the loss of the mitochondrial membrane potential was similar to the degree of cell death in hepatocytes from C57BL/6N and C57BL/6J mice. This confirmed that mitochondrial dysfunction is an established aspect of APAP-induced cell death *in vitro* in both murine hepatocytes (Bajt et al., 2004), in metabolically competent hepatoma cells (HepaRG) (McGill et al., 2011) and in primary human hepatocytes (Xie et al., 2014). Although we could document an initial higher susceptibility to APAP-induced mitochondrial dysfunction in hepatocytes isolated from C57BL/6N mice, the differences between hepatocytes of the two sub-strains disappeared when cells from the C57BL/6J sub-strain caught up with the injury mechanism several hours later. These findings further support the conclusions from the *in vivo* experiments that there are similar mechanisms of APAP toxicity in both sub-strains; it may require lower doses to observe permanent differences in

hepatocytes from C57BL/6N versus C57BL/6J mice. Nevertheless, a more detailed assessment of the mitochondrial bioenergetics is warranted. A similar phenomenon was previously seen *in vivo* when liver injury was only prevented in cyclophilin D-deficient mice after a low overdose of APAP (Ramachandran et al., 2011) but not after a higher dose (LoGuidice and Bolesterli, 2011) suggesting that the MPT pore opening can only be regulated by cyclophilin D during a lower cellular stress. However, this mechanism can be overwhelmed with higher doses leading to an unregulated MPT pore formation.

4.3 Sub-strain differences in biological research

A number of differences in basic physiology have previously been established between C57BL/6N and C57BL/6J mice (Fontaine and Davis, 2016; Simon et al., 2013). These differences were attributed to mediate the surprising changes between supposedly similar knockout mice in other models of disease (Newberry et al., 2015). The absence of the mitochondrial protein Nicotinamide Nucleotide Transhydrogenase (NNT) has routinely been suspected to be a major mediator in these differences (Freeman et al., 2006; Simon et al., 2013). Previously it was hypothesized that since NNT is responsible for interconversion of NADH to NADPH, it may be important for GSH regeneration from GSSG (Bourdi et al., 2011). However, we found no differences in GSH regeneration, indicating that interconversion of NADPH and NADH is of limited relevance for normal GSH re-synthesis in the APAP model and enhanced capacity for the generation of NADPH from NADH confers no advantage after APAP overdose. Thus, the *Nnt*-deficiency in C57BL/6J mice cannot explain the lower susceptibility to APAP hepatotoxicity in these animals.

This is in agreement with the previous observation showing that in the concanavalin A-induced liver injury model, C57BL/6N mice were more susceptible than C57BL/6J mice to APAP-induced liver injury (Bourdi et al., 2011) suggesting that the susceptibility difference between C57BL/6J and C57BL/6N is not necessarily dependent on drug metabolism but may be more dependent on the mitochondrial oxidant stress. Indeed, mitochondrial oxidative stress plays a pathologic role in the concanavalin A liver injury model (Ni et al., 2008). However, more detailed investigations are needed to evaluate the mechanisms of the different susceptibilities in various liver injury models between C57BL/6N and C57BL/6J mice.

The use of genetic knockout models has steadily increased since their inception and now represents the gold-standard in assessing the pathophysiological role of specific genes. While the use of gene knockout mice has led to a number of breakthroughs, potential pitfalls are present when the gene-deficient mice are not compared to the proper wild type animals (Fontaine and Davis, 2016; Vanden Berghe et al., 2015). Significant genetic drift has occurred in the C57BL/6 mouse sub-strains since the original split when a portion of the line from Jackson Labs was sent to the National Institutes of Health (Zurita et al., 2011). While this study did not directly identify the genetic differences mediating the increased susceptibility, it is clear that C57BL/6N mice experience increased APAP-protein adduct formation, increased mitochondrial dysfunction, and increased cell death after APAP overdose.

4.4 Conclusions

Overall, our data support a hypothesis where increased APAP-protein adduct formation in the C57BL/6N mouse causes enhanced phospho-JNK translocation to the mitochondria and enhanced BAX-mediated mitochondrial instability, which leads to more mitochondrial oxidative stress, and increased AIF and SMAC release. These differences result in more cell death and liver injury in C57BL/6N compared to C57BL/6J mice. These data strongly suggest that careful attention must be paid to the genetic differences between C57BL/6N and C57BL/6J during the generation of knockout models as insufficient back-crossing may yield results that are not specific to the gene in question.

Supplementary Material

Refer to Web version on PubMed Central for supplementary material.

5. ACKNOWLEDGEMENTS

This work was supported in part by the National Institutes of Health grants R01 AA12916, and R01 DK102142 and by grants from the National Center for Research Resources (5P20RR021940-07) and the National Institute of General Medical Sciences (8 P20 GM103549-07) of the National Institutes of Health. Additional support came from the “Training Program in Environmental Toxicology” T32 ES007079-26A2 (to B.L.W.) from the National Institute of Environmental Health Sciences.

Abbreviations

APAP	acetaminophen
AIF	apoptosis-inducing factor
ALT	alanine aminotransferase
ASK-1	apoptosis signal-regulating kinase 1
CYP	cytochrome P450
7-EFC	7-ethoxy-4-trifluoromethylcoumarin
HMGB1	high mobility group box 1
HPLC-ED	high performance liquid chromatography with electrochemical detection
KO mice	knockout mice
MLK-3	mixed lineage kinase-3
NAPQI	N-acetyl-p-benzoquinone imine
NNT	nicotinamide nucleotide transhydrogenase
MPT	mitochondrial permeability transition
JNK	c-jun *N*-terminal kinase
GSH	reduced glutathione

GSSG	glutathione disulfide
Sab	SH3BP5 binding protein
SMAC	second mitochondria-derived activator of caspases
SOD2	superoxide dismutase 2
Trx2	thioredoxin 2
TUNEL	terminal deoxynucleotidyl transferase (TdT) dUTP nick-end labeling assay

REFERENCES

Antoine DJ, Dear JW, Lewis PS, Platt V, Coyle J, Masson M, Thanacoody RH, Gray AJ, Webb DJ, Moggs JG, Bateman DN, Goldring CE, Park BK. Mechanistic biomarkers provide early and sensitive detection of acetaminophen-induced acute liver injury at first presentation to hospital. Hepatology. 2013; 58:777–787. [PubMed: 23390034]

Antoine DJ, Jenkins RE, Dear JW, Williams DP, McGill MR, Sharpe MR, Craig DG, Simpson KJ, Jaeschke H, Park BK. Molecular forms of HMGB1 and keratin-18 as mechanistic biomarkers for mode of cell death and prognosis during clinical acetaminophen hepatotoxicity. J. Hepatol. 2012; 56:1070–1079. [PubMed: 22266604]

Bajt ML, Cover C, Lemasters JJ, Jaeschke H. Nuclear translocation of endonuclease G and apoptosis-inducing factor during acetaminophen-induced liver cell injury. Toxicol. Sci. 2006; 94:217–225. [PubMed: 16896059]

Bajt ML, Farhood A, Lemasters JJ, Jaeschke H. Mitochondrial bax translocation accelerates DNA fragmentation and cell necrosis in a murine model of acetaminophen hepatotoxicity. J. Pharmacol. Exp. Ther. 2008; 324:8–14. [PubMed: 17906064]

Bajt ML, Knight TR, Lemasters JJ, Jaeschke H. Acetaminophen-induced oxidant stress and cell injury in cultured mouse hepatocytes: protection by N-acetyl cysteine. Toxicol. Sci. 2004; 80:343–349. [PubMed: 15115886]

Bajt ML, Ramachandran A, Yan HM, Lebofsky M, Farhood A, Lemasters JJ, Jaeschke H. Apoptosis-inducing factor modulates mitochondrial oxidant stress in acetaminophen hepatotoxicity. Toxicol. Sci. 2011; 122:598–605. [PubMed: 21572097]

Beger RD, Bhattacharyya S, Yang X, Gill PS, Schnackenberg LK, Sun J, James LP. Translational biomarkers of acetaminophen-induced acute liver injury. Arch. Toxicol. 2015; 89:1497–1522. [PubMed: 25983262]

Bessems JG, Vermeulen NP. Paracetamol (acetaminophen)-induced toxicity: molecular and biochemical mechanisms, analogues and protective approaches. Crit Rev Toxicol. 2001; 31:55–138. [PubMed: 11215692]

Bourdi M, Davies JS, Pohl LR. Mispairing C57BL/6 substrains of genetically engineered mice and wild-type controls can lead to confounding results as it did in studies of JNK2 in acetaminophen and concanavalin A liver injury. Chem. Res. Toxicol. 2011; 24:794–796. [PubMed: 21557537]

Bourdi M, Korrapati MC, Chakraborty M, Yee SB, Pohl LR. Protective role of c-Jun N-terminal kinase 2 in acetaminophen-induced liver injury. Biochem. Biophys. Res. Commun. 2008; 374:6–10. [PubMed: 18586006]

Buters JT, Schiller CD, Chou RC. A highly sensitive tool for the assay of cytochrome P450 enzyme activity in rat, dog and man. Direct fluorescence monitoring of the deethylation of 7-ethoxy-4-trifluoromethylcoumarin. Biochem. Pharmacol. 1993; 46:1577–1584. [PubMed: 8240414]

Cover C, Mansouri A, Knight TR, Bajt ML, Lemasters JJ, Pessayre D, Jaeschke H. Peroxynitrite-induced mitochondrial and endonuclease-mediated nuclear DNA damage in acetaminophen hepatotoxicity. J. Pharmacol. Exp. Ther. 2005; 315:879–887. [PubMed: 16081675]

Cohen SD, Pumford NR, Khairallah EA, Boekelheide K, Pohl LR, Amouzadeh HR, Hinson JA. Selective protein covalent binding and target organ toxicity. Toxicol. Appl. Pharmacol. 1997; 143:1–12. [PubMed: 9073586]

Dahlin DC, Miwa GT, Lu AY, Nelson SD. N-acetyl-p-benzoquinone imine: a cytochrome P-450-mediated oxidation product of acetaminophen. Proc. Natl. Acad. Sci. U. S. A. 1984; 81:1327–1331. [PubMed: 6424115]

Fontaine DA, Davis DB. Attention to background strain is essential for metabolic research: C57BL/6 and the International Knockout Mouse Consortium. Diabetes. 2016; 65:25–33. [PubMed: 26696638]

Freeman HC, Hugill A, Dear NT, Ashcroft FM, Cox RD. Deletion of nicotinamide nucleotide transhydrogenase: a new quantitive trait locus accounting for glucose intolerance in C57BL/6J mice. Diabetes. 2006; 55:2153–2156. [PubMed: 16804088]

Gujral JS, Knight TR, Farhood A, Bajt ML, Jaeschke H. Mode of cell death after acetaminophen overdose in mice: apoptosis or oncotic necrosis? Toxicol. Sci. 2002; 67:322–328. [PubMed: 12011492]

Gunawan BK, Liu ZX, Han D, Hanawa N, Gaarde WA, Kaplowitz N. c-Jun N-terminal kinase plays a major role in murine acetaminophen hepatotoxicity. Gastroenterology. 2006; 131:165–178. [PubMed: 16831600]

Han D, Dara L, Win S, Than TA, Yuan L, Abbasi SQ, Liu ZX, Kaplowitz N. Regulation of drug-induced liver injury by signal transduction pathways: critical role of mitochondria. Trends Pharmacol. Sci. 2013; 34:243–253. [PubMed: 23453390]

Hanawa N, Shinohara M, Saberi B, Gaarde WA, Han D, Kaplowitz N. Role of JNK translocation to mitochondria leading to inhibition of mitochondria bioenergetics in acetaminophen-induced liver injury. J. Biol. Chem. 2008; 283:13565–13577. [PubMed: 18337250]

Harrill AH, Ross PK, Gatti DM, Threadgill DW, Rusyn I. Population-based discovery of toxicogenomics biomarkers for hepatotoxicity using a laboratory strain diversity panel. Toxicol. Sci. 2009a; 110:235–243. [PubMed: 19420014]

Harrill AH, Watkins PB, Su S, Ross PK, Harbourt DE, Stylianou IM, Boorman GA, Russo MW, Sackler RS, Harris SC, Smith PC, Tennant R, Bogue M, Paigen K, Harris C, Contractor T, Wiltshire T, Rusyn I, Threadgill DW. Mouse population-guided resequencing reveals that variants in CD44 contribute to acetaminophen-induced liver injury in humans. Genome Res. 2009b; 19:1507–1515. [PubMed: 19416960]

Henderson NC, Pollock KJ, Frew J, Mackinnon AC, Flavell RA, Davis RJ, Sethi T, Simpson KJ. Critical role of c-jun (NH2) terminal kinase in paracetamol-induced acute liver failure. Gut. 2007; 56:982–990. [PubMed: 17185352]

Hu J, Ramshesh VK, McGill MR, Jaeschke H, Lemasters JJ. Low dose acetaminophen induces reversible mitochondrial dysfunction associated with transient c jun N-terminal kinase activation in mouse liver. Toxicol. Sci. 2016; 150:204–215. [PubMed: 26721299]

Jaeschke H. Glutathione disulfide formation and oxidant stress during acetaminophen-induced hepatotoxicity in mice in vivo: the protective effect of allopurinol. J. Pharmacol. Exp. Ther. 1990; 255:935–941. [PubMed: 2262912]

Jaeschke H, McGill MR, Ramachandran A. Oxidant stress, mitochondria, and cell death mechanisms in drug-induced liver injury: lessons learned from acetaminophen hepatotoxicity. Drug Metab. Rev. 2012; 44:88–106. [PubMed: 22229890]

Jaeschke H, Mitchell JR. Use of isolated perfused organs in hypoxia and ischemia/reperfusion oxidant stress. Methods Enzymol. 1990; 186:752–759. [PubMed: 2233332]

Jollow DJ, Mitchell JR, Potter WZ, Davis DC, Gillette JR, Brodie BB. Acetaminophen-induced hepatic necrosis. II. Role of covalent binding in vivo. J. Pharmacol. Exp. Ther. 1973; 187:195–202. [PubMed: 4746327]

Kon K, Kim JS, Jaeschke H, Lemasters JJ. Mitochondrial permeability transition in acetaminophen-induced necrosis and apoptosis of cultured mouse hepatocytes. Hepatology. 2004; 40:1170–1179. [PubMed: 15486922]

Lee WM. Drug-induced acute liver failure. Clin. Liver Dis. 2013; 17:575–586. [PubMed: 24099019]

LoGuidice A, Boelsterli UA. Acetaminophen overdose-induced liver injury in mice is mediated by peroxynitrite independently of the cyclophilin D-regulated permeability transition. Hepatology. 2011; 54:969–978. [PubMed: 21626531]

McGill MR, Jaeschke H. Metabolism and disposition of acetaminophen: recent advances in relation to hepatotoxicity and diagnosis. Pharm. Res. 2013; 30:2174–2187. [PubMed: 23462933]

McGill MR, Jaeschke H. Mechanistic biomarkers in acetaminophen-induced hepatotoxicity and acute liver failure: from preclinical models to patients. Expert Opin. Drug Metab. Toxicol. 2014; 10:1005–1017. [PubMed: 24836926]

McGill MR, Lebofsky M, Norris HR, Slawson MH, Bajt ML, Xie Y, Williams CD, Wilkins DG, Rollins DE, Jaeschke H. Plasma and liver acetaminophen-protein adduct levels in mice after acetaminophen treatment: dose-response, mechanisms, and clinical implications. Toxicol. Appl. Pharmacol. 2013; 269:240–249. [PubMed: 23571099]

McGill MR, Sharpe MR, Williams CD, Taha M, Curry SC, Jaeschke H. The mechanism underlying acetaminophen-induced hepatotoxicity in humans and mice involves mitochondrial damage and nuclear DNA fragmentation. J. Clin. Invest. 2012; 122:1574–1583. [PubMed: 22378043]

McGill MR, Staggs VS, Sharpe MR, Lee WM, Jaeschke H, Acute Liver Failure Study Group. Serum mitochondrial biomarkers and damage-associated molecular patterns are higher in acetaminophen overdose patients with poor outcome. Hepatology. 2014; 60:1336–1345. [PubMed: 24923598]

McGill MR, Yan HM, Ramachandran A, Murray GJ, Rollins DE, Jaeschke H. HepaRG cells: a human model to study mechanisms of acetaminophen hepatotoxicity. Hepatology. 2011; 53:974–982. [PubMed: 21319200]

Mitchell JR, Jollow DJ, Potter WZ, Davis DC, Gillette JR, Brodie BB. Acetaminophen-induced hepatic necrosis. I. Role of drug metabolism. J. Pharmacol. Exp. Ther. 1973a; 187:185–194. [PubMed: 4746326]

Mitchell JR, Jollow DJ, Potter WZ, Gillette JR, Brodie BB. Acetaminophen-induced hepatic necrosis. IV. Protective role of glutathione. J. Pharmacol. Exp. Ther. 1973b; 187:211–217. [PubMed: 4746329]

Muldrew KL, James LP, Coop L, McCullough SS, Hendrickson HP, Hinson JA, Mayeux PR. Determination of acetaminophen-protein adducts in mouse liver and serum and human serum after hepatotoxic doses of acetaminophen using high-performance liquid chromatography with electrochemical detection. Drug Metab. Dispos. 2002; 30:446–451. [PubMed: 11901099]

Nelson SD. Molecular mechanisms of the hepatotoxicity caused by acetaminophen. Semin. Liver Dis. 1990; 10:267–278. [PubMed: 2281334]

Newberry EP, Kennedy S, Xie Y, Luo J, Jiang H, Ory DS, Davidson NO. Phenotypic divergence in two lines of L-Fabp−/− mice reflects substrain differences and environmental modifiers. Am. J. Physiol. Gastrointest. Liver Physiol. 2015; 309:G648–661. [PubMed: 26251469]

Ni HM, Bockus A, Boggess N, Jaeschke H, Ding WX. Activation of autophagy protects against acetaminophen-induced hepatotoxicity. Hepatology. 2012a; 55:222–232. [PubMed: 21932416]

Ni HM, Boggess N, McGill MR, Lebofsky M, Borude P, Apte U, Jaeschke H, Ding WX. Liver-specific loss of Atg5 causes persistent activation of Nrf2 and protects against acetaminophen-induced liver injury. Toxicol. Sci. 2012b; 127:438–450. [PubMed: 22491424]

Ni HM, Chen X, Ding WX, Schuchmann M, Yin XM. Differential roles of JNK in ConA/GalN and ConA-induced liver injury in mice. Am. J. Pathol. 2008; 173:962–972. [PubMed: 18772342]

Ni HM, McGill MR, Chao X, Du K, Williams JA, Xie Y, Jaeschke H, Ding WX. Removal of acetaminophen protein adducts by autophagy protects against acetaminophen-induced liver injury in mice. J. Hepatol. 2016; 65:354–362. [PubMed: 27151180]

Ramachandran A, Lebofsky M, Baines CP, Lemasters JJ, Jaeschke H. Cyclophilin D deficiency protects against acetaminophen-induced oxidant stress and liver injury. Free Radic. Res. 2011; 45:156–164. [PubMed: 20942566]

Ray SD, Sorge CL, Raucy JL, Corcoran GB. Early loss of large genomic DNA in vivo with accumulation of Ca2+ in the nucleus during acetaminophen-induced liver injury. Toxicol. Appl. Pharmacol. 1990; 106:346–351. [PubMed: 2256122]

Rosen GM, Rauckman EJ, Ellington SP, Dahlin DC, Christie JL, Nelson SD. Reduction and glutathione conjugation reactions of N-acetyl-p-benzoquinone imine and two dimethylated analogues. Mol. Pharmacol. 1984; 25:151–157. [PubMed: 6323948]

Saito C, Lemasters JJ, Jaeschke H. c-Jun N-terminal kinase modulates oxidant stress and peroxynitrite formation independent of inducible nitric oxide synthase in acetaminophen hepatotoxicity. Toxicol. Appl. Pharmacol. 2010; 246:8–17. [PubMed: 20423716]

Sharma M, Gadang V, Jaeschke A. Critical role for mixed-lineage kinase 3 in acetaminophen-induced hepatotoxicity. Mol. Pharmacol. 2012; 82:1001–1007. [PubMed: 22918968]

Simon MM, Greenaway S, White JK, Fuchs H, Gailus-Durner V, Wells S, Sorg T, Wong K, Bedu E, Cartwright EJ, Dacquin R, Djebali S, Estabel J, Graw J, Ingham NJ, Jackson IJ, Lengeling A, Mandillo S, Marvel J, Meziane H, Preitner F, Puk O, Roux M, Adams DJ, Atkins S, Ayadi A, Becker L, Blake A, Brooker D, Cater H, Champy MF, Combe R, Danecek P, di Fenza A, Gates H, Gerdin AK, Golini E, Hancock JM, Hans W, Hölter SM, Hough T, Jurdic P, Keane TM, Morgan H, Müller W, Neff F, Nicholson G, Pasche B, Roberson LA, Rozman J, Sanderson M, Santos L, Selloum M, Shannon C, Southwell A, Tocchini-Valentini GP, Vancollie VE, Westerberg H, Wurst W, Zi M, Yalcin B, Ramirez-Solis R, Steel KP, Mallon AM, de Angelis MH, Herault Y, Brown SD. A comparative phenotypic and genomic analysis of C57BL/6J and C57BL/6N mouse strains. Genome Biol. 2013; 14:R82. [PubMed: 23902802]

Tirmenstein MA, Nelson SD. Subcellular binding and effects on calcium homeostasis produced by acetaminophen and a nonhepatotoxic regioisomer, 3'-hydroxyacetanilide, in mouse liver. J. Biol. Chem. 1989; 264:9814–9819. [PubMed: 2524496]

Vanden Berghe T, Hulpiau P, Martens L, Vandenbroucke RE, Van Wonterghem E, Perry SW, Bruggeman I, Divert T, Choi SM, Vuylsteke M, Shestopalov VI, Libert C, Vandenabeele P. Passenger mutations confound interpretation of all genetically modified congenic mice. Immunity. 2015; 43:200–209. [PubMed: 26163370]

Win S, Than TA, Han D, Petrovic LM, Kaplowitz N. c-Jun N-terminal kinase (JNK)-dependent acute liver injury from acetaminophen or tumor necrosis factor (TNF) requires mitochondrial Sab protein expression in mice. J. Biol. Chem. 2011; 286:35071–35078. [PubMed: 21844199]

Xie Y, McGill MR, Dorko K, Kumer SC, Schmitt TM, Forster J, Jaeschke H. Mechanisms of acetaminophen-induced cell death in primary human hepatocytes. Toxicol. Appl. Pharmacol. 2014; 279:266–274. [PubMed: 24905542]

Xie Y, McGill MR, Du K, Dorko K, Kumer SC, Schmitt TM, Ding WX, Jaeschke H. Mitochondrial protein adducts formation and mitochondrial dysfunction during N-acetyl-m-aminophenol (AMAP)-induced hepatotoxicity in primary human hepatocytes. Toxicol. Appl. Pharmacol. 2015a; 289:213–222. [PubMed: 26431796]

Xie Y, Ramachandran A, Breckenridge DG, Liles JT, Lebofsky M, Farhood A, Jaeschke H. Inhibitor of apoptosis signal-regulating kinase 1 protects against acetaminophen-induced liver injury. Toxicol. Appl. Pharmacol. 2015b; 286:1–9. [PubMed: 25818599]

Zaher H, Buters JT, Ward JM, Bruno MK, Lucas AM, Stern ST, Cohen SD, Gonzalez FJ. Protection against acetaminophen toxicity in CYP1A2 and CYP2E1 double-null mice. Toxicol. Appl. Pharmacol. 1998; 152:193–199. [PubMed: 9772215]

Zurita E, Chagoyen M, Cantero M, Alonso R, González-Neira A, López-Jiménez A, López-Moreno JA, Landel CP, Benítez J, Pazos F, Montoliu L. Genetic polymorphisms among C57BL/6 mouse inbred strains. Transgenic Res. 2011; 20:481–489. [PubMed: 20506040]

HIGHLIGHTS

- Acetaminophen (APAP) hepatotoxicity is more severe in C57BL/6N versus C57BL/6J mice
- C57BL/6N have increased mitochondrial APAP protein adducts compared to C57BL/6J mice
- C57BL/6N mice show increased mitochondrial dysfunction and higher DNA fragmentation
- APAP hepatotoxicity mechanisms are similar between the 6N and the 6J sub-strains
- Overall, C57BL/6N mice are more susceptible to APAP overdose

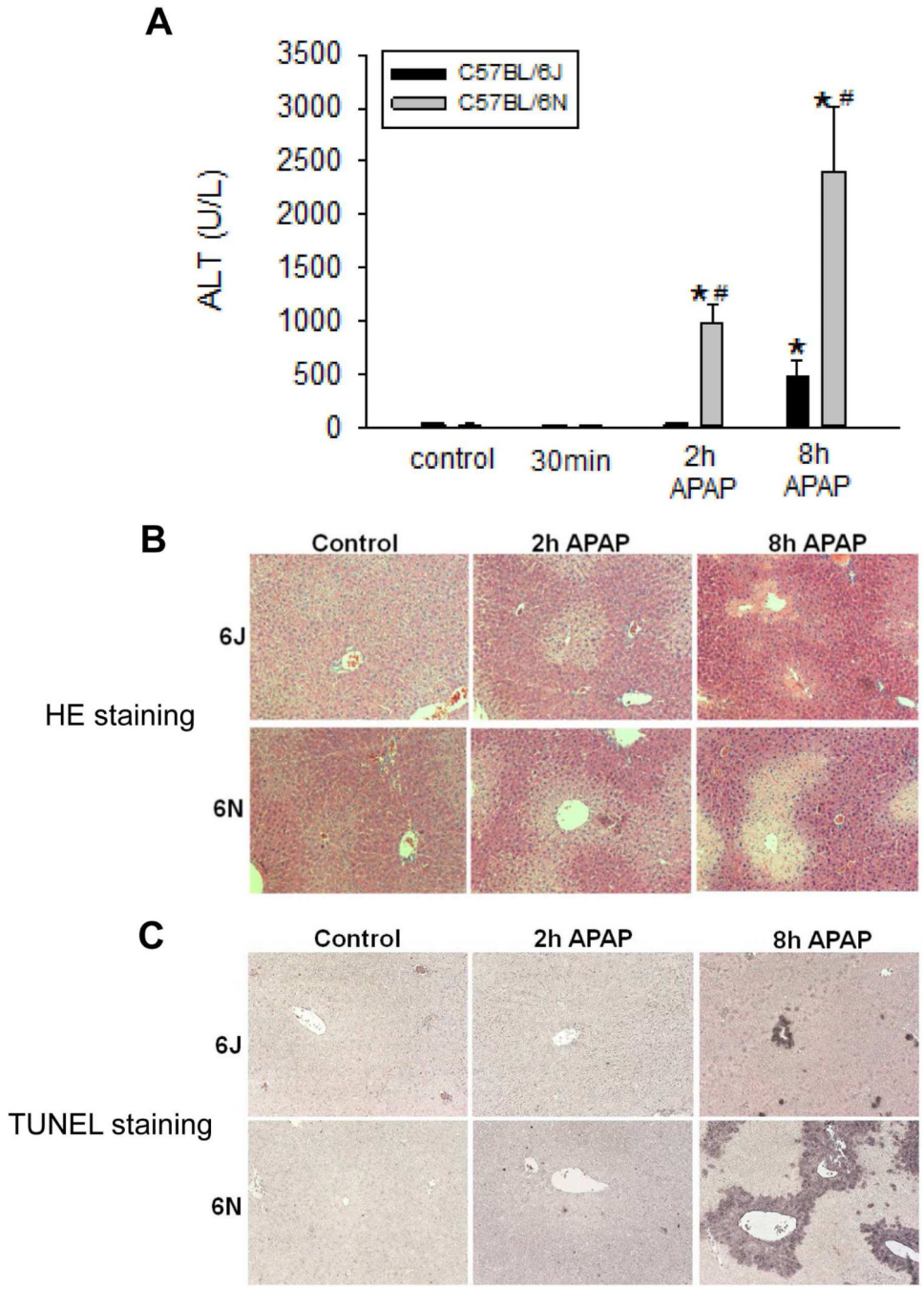

Figure 1.

Acetaminophen-induced liver injury in C57BL/6J and C57BL/6N mice. Animals were treated with 200 mg/kg APAP or saline as control. (A) Plasma ALT activities of C57BL/6J and C57BL/6N mice at 0.5, 2, and 8 h. (B) Representative H&E-stained liver section (×50 magnification) and (C) TUNEL staining (×50 magnification) are shown for controls and animals treated with APAP for 2 h and 8 h. Data represent means ± SE of n=4 animals per group. *$p < 0.05$ (compared with controls, $t=0$). #$p < 0.05$ (compared with C57BL/6J mice treated with APAP).

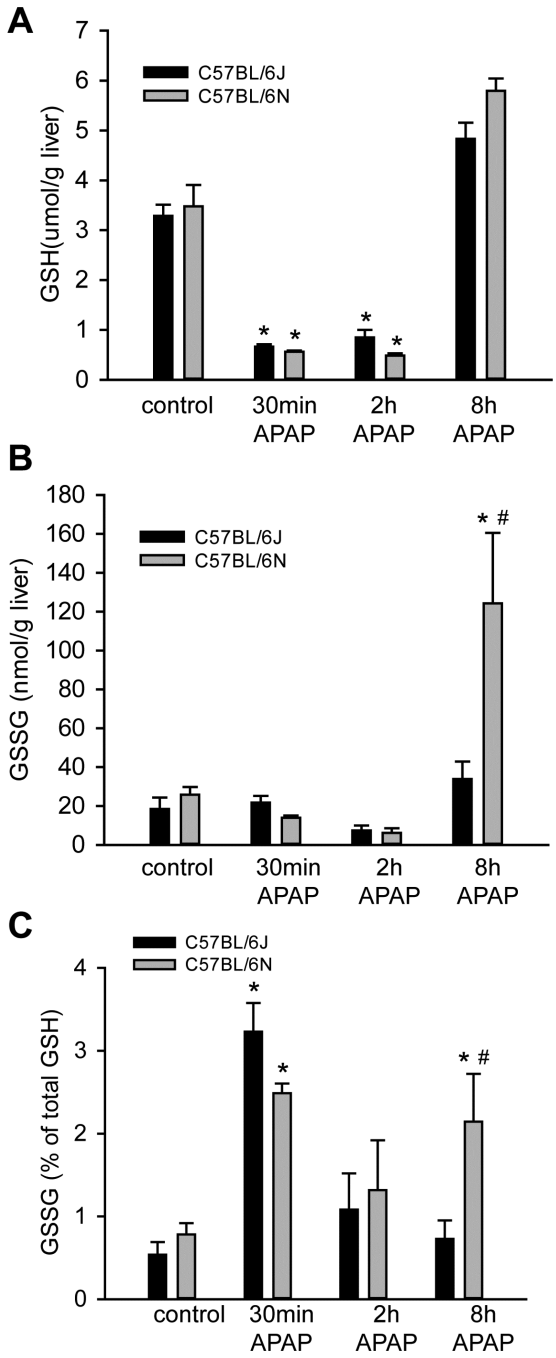

Figure 2.

Liver GSH and GSSG content after APAP treatment. C57BL/6J and C57BL/6N mice were treated with 200 mg/kg APAP or saline as control. Total GSH (A) was measured in liver tissue homogenate at 0.5, 2 and 8 h post-APAP and in control mice. GSSG was measured at the same times in C57BL/6J and C57BL/6N mice (B) and the percent of GSSG compared to total GSH was calculated (C). Data represent means ± SE of n=4 animals per group. *$p<$ 0.05 (compared with controls, t=0). #$p<$ 0.05 (compared with C57BL/6J mice treated with APAP).

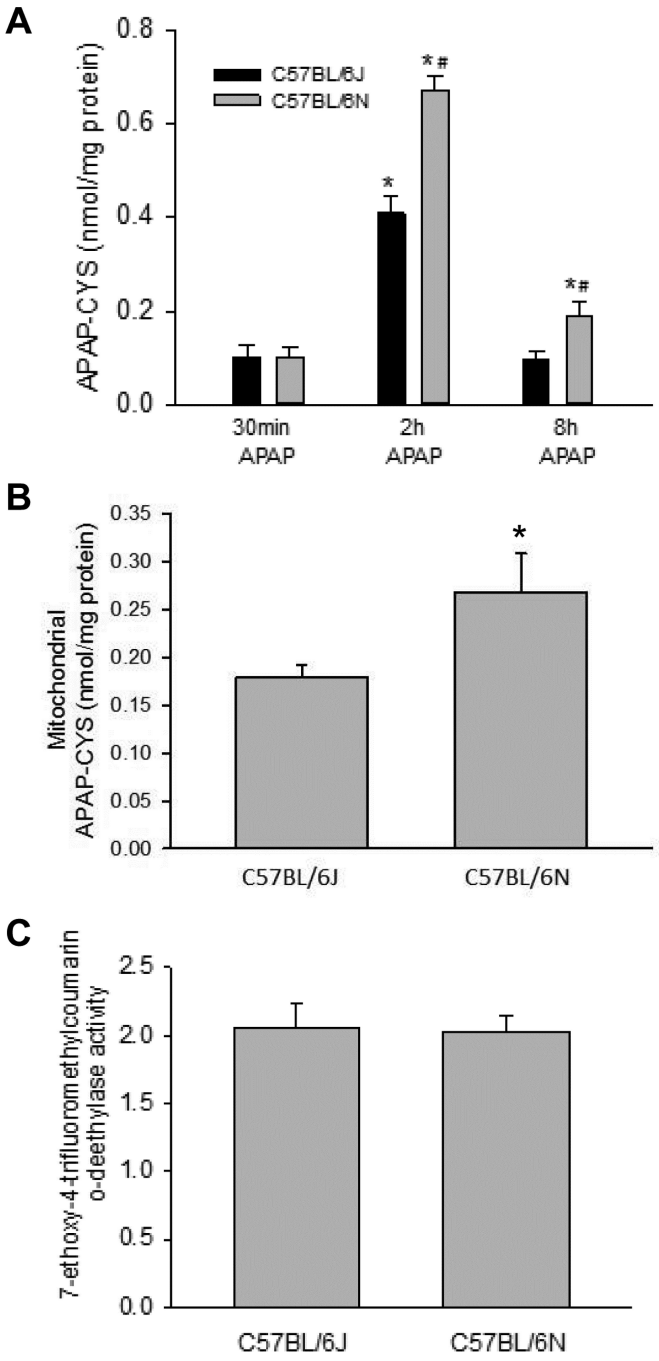

Figure 3.

APAP-protein adduct formation and P450 activities in C57BL/6J and C57BL/6N mice. C57BL/6J and C57BL/6N mice were treated with 200 mg/kg APAP or saline as control. APAP-cysteine adducts were quantified by HPLC-ED in liver homogenate at 30 min, 2h and 8h post-APAP (A) or mitochondria (B) at 2 h post-APAP (peak of adduct formation) in C57BL/6J and C57BL/6N mice. Cytochrome P450 activities were measured in the 14,000×g supernatant of control mouse liver homogenate using the 7EFC deethylase assay (C). Data

represent means ± SE of n=4 animals per group. *$p < 0.05$ (compared with C57BL/6J mice, $t=0$).

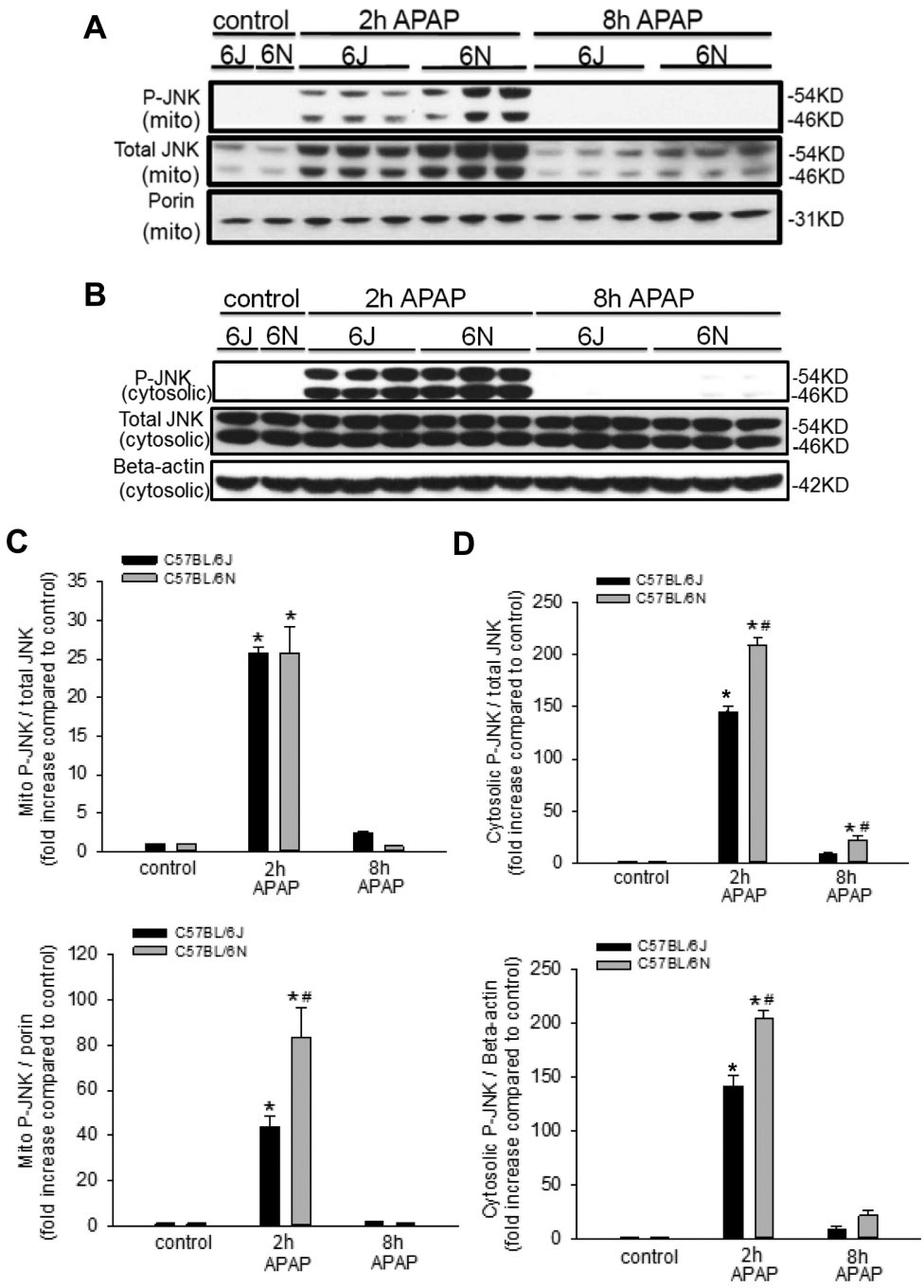

Figure 4.

JNK phosphorylation in liver cytosolic fraction and mitochondrial p-JNK translocation after APAP treatment in C57BL/6J and C57BL/6N mice. Animals were treated with 200 mg/kg APAP or saline as control. At 2 h and 8 h after APAP, cytosolic and mitochondrial fractions were subjected to western blotting for phosphorylated JNK, total JNK, porin and beta-actin (A and B). Densitometry was performed on these blots and the pJNK-to-JNK ratio, the pJNK-to-beta actin ratio and pJNK-to-Porin ratio was calculated for the different time points of C57BL/6J and C57BL/6N mice Data represent mean ± SE of n=3 animals per group. *p<

0.05 (compared with controls, t=0). #p< 0.05 (compared with C57BL/6J mice treated with APAP).

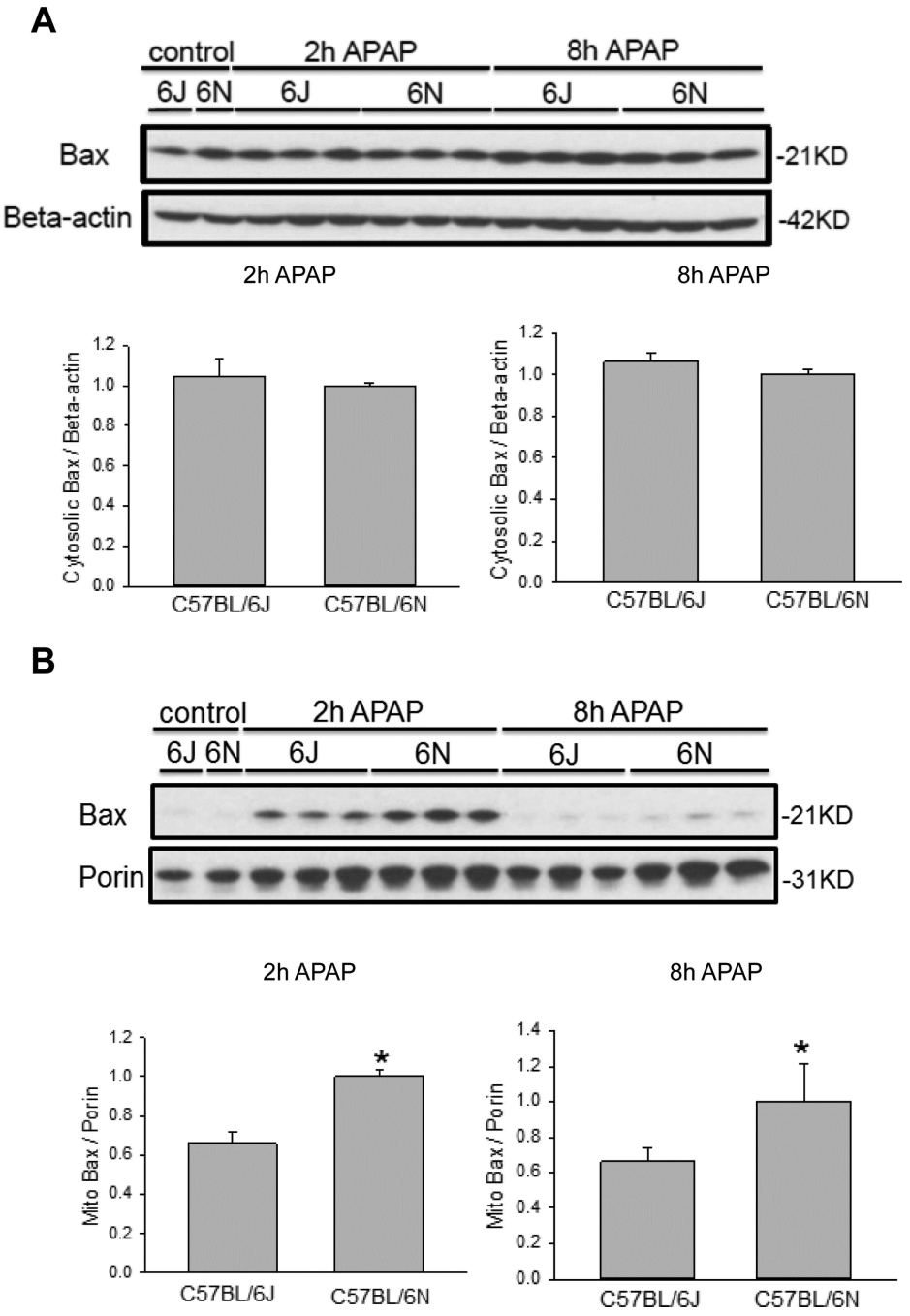

Figure 5.

Mitochondrial BAX translocation after APAP treatment in C57BL/6J and C57BL/6N mice. Animals were treated with 200 mg/kg APAP or saline as control. At 2 h and 8 h after APAP, cytosolic fractions were subjected to western blotting for BAX and beta-actin (A). Western blotting was also performed on the isolated mitochondrial fraction for BAX and porin (B). Densitometry was performed on these blots and the cytosolic BAX-to-beta actin and the mitochondrial BAX-to-porin ratio was calculated for the different time points of C57BL/6J and C57BL/6N mice. The cytosolic or mitochondrial ratio for each time point for the 6N

strain was set to 1 and the corresponding ratios for the 6J strain were expressed as a fraction of 1. Data represent means ± SE of n=3 animals per group. *$p < 0.05$ (compared with C57BL/6J mice, $t=0$).

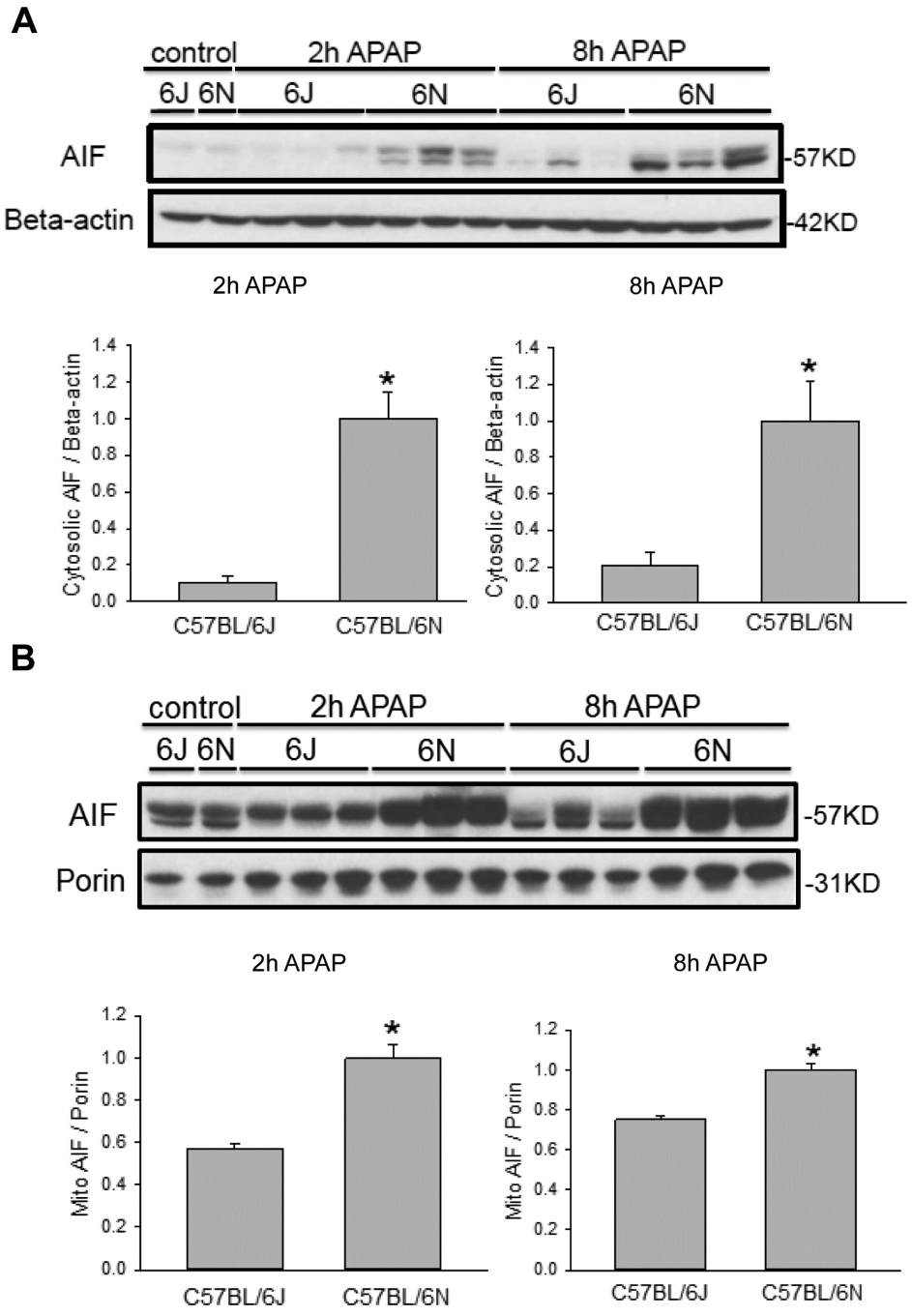

Figure 6.

Mitochondrial AIF release after APAP treatment in C57BL/6J and C57BL/6N mice. Animals were treated with 200 mg/kg APAP or saline as control. At 2 h and 8 h after APAP, cytosolic fractions were subjected to western blotting for AIF and beta-actin (A). Western blotting was also performed on the isolated mitochondrial fraction for AIF and porin (B). Densitometry was performed on these blots and the cytosolic AIF-to-beta actin and the mitochondrial AIF-to-porin ratio was calculated for the different time points of C57BL/6J and C57BL/6N mice. The cytosolic or mitochondrial ratio for each time point for the 6N

strain was set to 1 and the corresponding ratios for the 6J strain were expressed as a fraction of 1. Data represent means ± SE of n=3 animals per group. *$p < 0.05$ (compared with C57BL/6J mice, $t=0$).

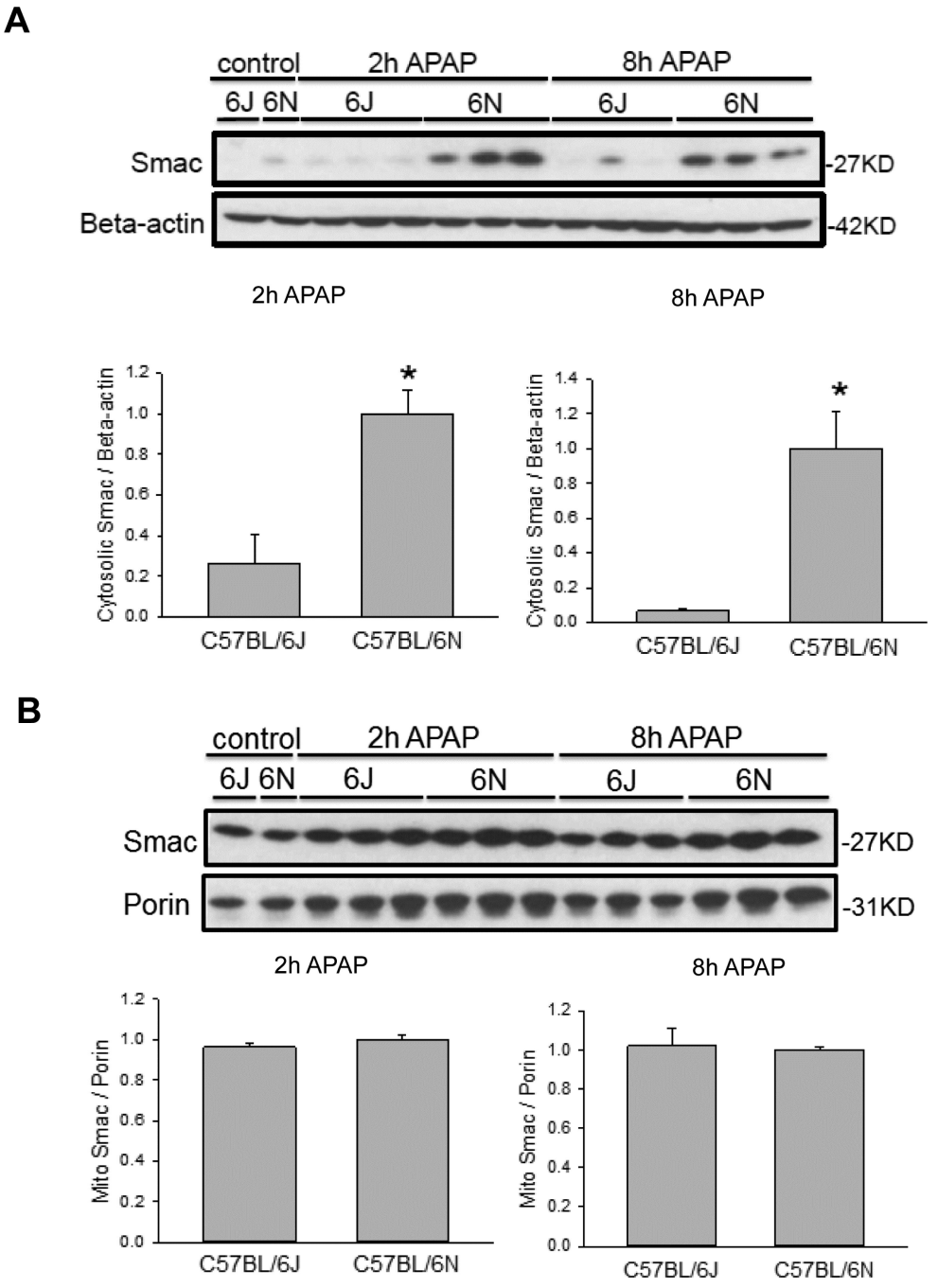

Figure 7.

Mitochondrial SMAC release after APAP treatment in C57BL/6J and C57BL/6N mice. Animals were treated with 200 mg/kg APAP or saline as control. At 2 h and 8 h after APAP, cytosolic fractions were subjected to western blotting for SMAC and ß-actin (A). Western blotting was also performed on the isolated mitochondrial fraction for SMAC and porin (B). Densitometry was performed on these blots and the cytosolic SMAC-to-beta actin and the mitochondrial SMAC-to-porin ratio was calculated for the different time points of C57BL/6J and C57BL/6N mice. The cytosolic or mitochondrial ratio for each time point for the 6N

strain was set to 1 and the corresponding ratios for the 6J strain were expressed as a fraction of 1. Data represent means ± SE of n=3 animals per group. *$p < 0.05$ (compared with C57BL/6J mice, $t=0$).

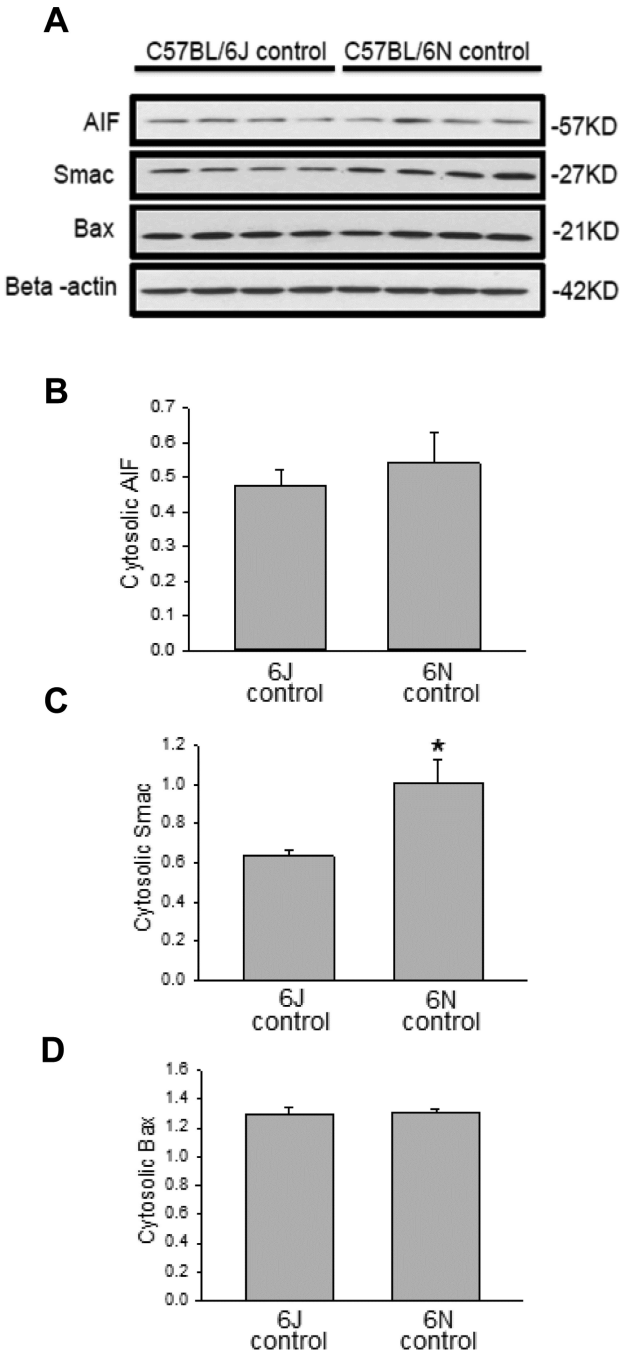

Figure 8.

Cytosolic baseline levels of AIF, SMAC and BAX in C57BL/6J and C57BL/6N mice. Using the control mice, cytosolic fractions were subjected to western blotting for AIF, SMAC and BAX (A). Densitometry was performed on these blots and the ratio of the protein-to-beta actin was calculated (B), (C), (D). Data represent mean ± SE of n=4 animals per group. *p< 0.05 (compared with C57BL/6J mice, t=0).

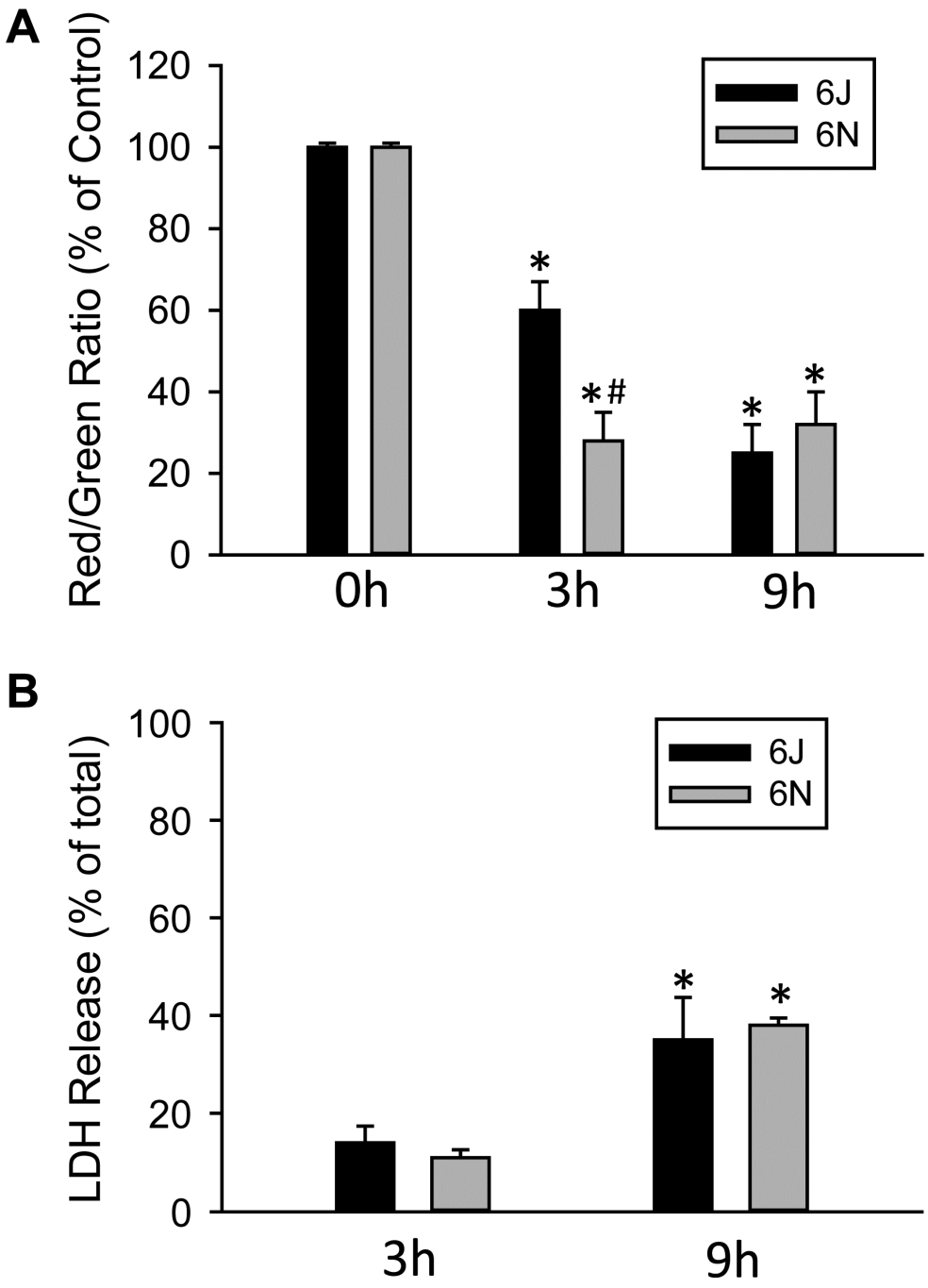

Figure 9.

Effect of APAP on mitochondrial function and viability in cells from C57BL/6J and C57BL/6N mice. Primary hepatocytes isolated from C57BL/6J and C57BL/6N mice were treated with media containing 5 mM APAP or control media. (A) Mitochondrial membrane potential, as indicated by the red/green fluorescence ratio, was determined with the JC-1 assay at 0, 3 and 9 h after 5 mM APAP. (B) Cell death, as indicated by the percentage of lactate dehydrogenase (LDH) released into the culture media, was assessed at 3 and 9 h after

APAP. Data represent mean ± SE of n = 4 cell isolations. *$p < 0.05$ (compared to untreated cells, t=0); $^{\#}p < 0.05$ (compared to cells from C57BL/6J mice).